Theory and Canonical Experiment Development for Strong Shock-Induced Droplet Drag and Vaporization

Nikolaos Kateris, Ethan S. Genter, Amitesh S. Jayaraman, Hai Wang
Mechanical Engineering Department, Stanford University
Stanford, California, United States

1 Introduction

Two-phase detonation physics involves the interaction of fuel droplets with detonation waves that are characterized by shocks of Mach number M$\sim$5. Shock impact is expected to cause catastrophic breakup and vaporization of fuel droplets, in large Weber number regimes (We $>$ 1000). Previous experimental investigations of shock-droplet interactions [1–4] have demonstrated that droplets impacted by sufficiently strong shocks undergo rapid flattening, followed by expansion and fast vaporization, with droplet vaporization time varying linearly with initial droplet diameter. The same behavior and linear relationship were confirmed for nanometer-sized droplets by molecular dynamics (MD) simulations [5]. Molecular dynamics [5] shed additional light on the momentum and energy transfer mechanisms from the post-shock flow to the fuel droplets: the post-shock flow impacts and deposits momentum and energy to fuel droplets by a direct gas impingement, or a *tachyothesis*, mechanism, leading to the rapid displacement and heating of the fuel. The fuel reaches a supercritical state, with diminishing surface tension, and the temperature of the fuel increases in a non-equilibrium process characterized by translational overheating, until the fuel reaches the post-shock thermodynamic state. In this work, we present a physics-based analytical theory to describe the coupled drag and vaporization of droplets upon shock-impact, based on the tachyothesis mechanism of momentum and energy deposition from the post-shock flow. The theory reproduces experimental and MD data with excellent agreement across different fuels, shock strengths, pre-shock thermodynamic states and droplet sizes. More importantly, we propose and test a canonical experiment targeting the determination of relevant physical parameters to enable the a priori prediction of droplet drag and vaporization for liquid fuels behind shocks. Specifically, experimental data are shown to inform a skin friction correction to droplet drag, and a droplet flattening shape response factor which impacts the rate of energy transfer from the post-shock flow to the fuel.

2 Drag and Vaporization Theory

Coupled momentum and energy transfer models are constructed to predict the acceleration of and energy deposition into the droplet upon shock impact, as illustrated in Fig. 1. Based on previous MD simulations [5], the dominant mechanisms of momentum and energy transfer are due to direct post-shock flow impact on the front surface of the droplet facing the shock, while negligible momentum and energy is

Correspondence to: nkateris@stanford.edu

transferred on the back side. The shock passage time is significantly shorter than all dynamic timescales of this problem. We assume full momentum and kinetic energy accommodation of the post-shock flow onto the droplet, which is justified by analyzing the MD velocity distribution of gas molecules in the vicinity of the droplet, which exchange their momentum with and deposit kinetic energy to the droplet with an accommodation coefficient of 84% and 92% respectively. The post-shock gas would transfer additional thermal energy to the droplet by convective heat transfer at a substantially slower rate; thus, this mechanism is not included here. Furthermore, relaxing the assumption of full kinetic energy accommodation and forming a bow shock yields only a minor delay in droplet vaporization. Lastly, we assume that the volume fraction of the droplets is low enough such that a negligible amount of momentum or energy is lost from the shock.

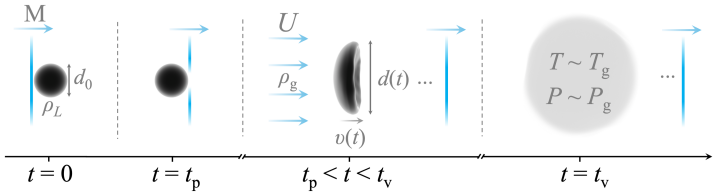

Figure 1: A droplet of (initial) density ρ_{L} and diameter d_0 is impacted by a shock of Mach number M at $t = 0$. The shock passes through the droplet at time t_{p}. The fuel then assumes a shape of circular projected area with changing diameter $d(t)$, moving with velocity $v(t)$. The compressed gas has free-stream speed U, density ρ_{g} and temperature T_{g}. At time $t = t_{\mathrm{v}}$ the fuel has reached the post-shock temperature and pressure (T_{g}, P_{g}).

We thus formulate an analytical coupled drag and vaporization model by considering a spherical droplet of initial diameter d_0 deforming (or pancaking) into a shape of circular projected area and propagating downstream with instantaneous speed $v(t)$, as illustrated in Fig. 1. The time-dependent diameter $d(t)$ can be represented by: $d(t) = d_0\,(1 + f)$, where $f(t)$ is a shape function that describes the time-dependent droplet deformation ($f(0) = 0$). For weak shocks and/or when the droplet-gas drift velocity is small, the droplet deformation can be impacted by viscous effects, and its amplification may be modeled by introducing a skin friction factor ϵ such that the effective radius becomes $d_{\mathrm{eff}}(t) = d_0\,(1 + f)\,(1 + \epsilon)$.

The drag model developed here considers frontal momentum deposition from the post-shock gas flow to the droplet, accelerating it from rest to the free-stream speed U in the lab frame. The equation of motion for a fuel droplet of mass m at a given rate of momentum transfer $\dot{M}$ is

$$\dot{M} = m\frac{\mathrm{d}v(t)}{\mathrm{d}t} = \frac{m}{\tau}[U - v(t)], \tag{1}$$

which results in a droplet speed $v(t)$ of the form $v(t) = U\left(1 - e^{-t/\tau}\right)$. In the above equation, τ is a velocity relaxation time scale. The momentum flux from the flow to the fuel is given by $\dot{M}'' = \rho_{\mathrm{g}}[U - v(t)]^2$, and therefore, the momentum transfer rate to the fuel is

$$\dot{M} = \rho_{\mathrm{g}}[U - v(t)]^2\frac{\pi}{4}\left[d_{\mathrm{eff}}(t)\right]^2 = \frac{\pi}{4}d_0^2\rho_{\mathrm{g}}[U - v(t)]^2\,(1 + f)^2\,(1 + \epsilon)^2. \tag{2}$$

Equating 1 and 2, letting $m = \rho_{\mathrm{L}}\frac{1}{6}\pi d_0^3$ and using the initial conditions $f(0) = 0$, and $v(0) = 0$, we find:

$$\tau = \frac{2}{3}\frac{\rho_{\mathrm{L}}}{\rho_{\mathrm{g}}}\frac{d_0}{U(1 + \epsilon)^2} \tag{3}$$

and

$$v(t) = U\left[1 - e^{-t/\left(\frac{2}{3}\frac{\rho_{\mathrm{L}}}{\rho_{\mathrm{g}}}\frac{d_0}{U(1+\epsilon)^2}\right)}\right]. \tag{4}$$

Integrating and non-dimensionalizing, we find the droplet displacement to be:

$$\frac{x(t)}{U\tau} = \frac{t}{\tau} + e^{-t/\tau} - 1. \tag{5}$$

The vaporization model considers the energy transfer from the post-shock flow to the fuel droplet undergoing deformation with the projected area diameter $d(t)$. Consistent with the momentum flux, the energy flux may be given by $\dot{E}'' = \frac{1}{2}\rho_{\mathrm{g}}(U - v(t))^3$ and the rate of energy transfer is:

$$\dot{E} = \frac{1}{2}\rho_{\mathrm{g}}[U - v(t)]^3\frac{\pi}{4}[d_{\mathrm{eff}}(t)]^2 = \frac{1}{8}\pi\rho_{\mathrm{g}}[U - v(t)]^3 d_0^2(1+f)^2(1+\epsilon)^2, \tag{6}$$

where ϵ accounts for skin friction effects as before. Vaporization time t_{v} is defined when enough energy is deposited into the droplet such that its specific enthalpy h is increased to that of its end state, defined when the droplet material is in thermodynamic equilibrium with the post-shock gas (T_{g}, P_{g}, U). Here, the change in enthalpy Δh is the sum of the heat of vaporization, Δh_{vap}, and the sensible enthalpy of vapor-phase fuel, Δh_{sens}. The increase in the total droplet energy to reach its end state at time t_{v} is:

$$\int_0^{t_{\mathrm{v}}} \dot{E}\mathrm{d}t = \rho_{\mathrm{L}}\frac{1}{6}\pi d_0^3\Delta h. \tag{7}$$

Combining eqs. 6 and 7 and simplifying, we find

$$\int_0^{t_{\mathrm{v}}} [U - v(t)]^3(1+f)^2\mathrm{d}t = \frac{4}{3}\frac{\rho_{\mathrm{L}}}{\rho_{\mathrm{g}}}\frac{\Delta h d_0}{(1+\epsilon)^2}. \tag{8}$$

Here we assume that the vaporization time varies linearly with the initial droplet diameter d_0, as discussed in section 1. We thus model the shape factor, $(1+f)$, as $(1+f) = \exp\left(\frac{\zeta+3}{2}\frac{t}{\tau}\right)$, which satisfies the initial condition ($f(0) = 0$). The parameter ζ is a shape response factor and determines the rate of flattening and expansion of the droplets as a result of mechanical work. Suffice it to note that ζ must be determined experimentally from the slope of a linear relationship between $\ln[d(t)/d_0]$ and the dimensionless time t/τ during early times of droplet deformation:

$$\ln\left[\frac{d(t)}{d_0}\right]_{t\to 0} = \frac{\zeta+3}{2}\frac{t}{\tau}. \tag{9}$$

Eq. 9 describes the shape evolution of the droplet at early times, when the term $(U - v)^3$ is large and energy transfer is most prominent. Hence, we obtain an expression for non-dimensional vaporization time by integrating Eq. 8:

$$\frac{t_{\mathrm{v}}}{\tau} = \frac{1}{\zeta}\ln\left(1 + \zeta\frac{\Delta h}{U^2/2}\right). \tag{10}$$

We therefore observe that the intrinsic vaporization time depends on the shape response factor, ζ, the momentum relaxation time, τ, and the ratio of enthalpy gain of the fuel to the kinetic energy of the incoming post-shock flow.

3 Results and Discussion

In typical experiments of shock-droplet interactions, the two key observables available to measurement are the spatial displacement of the center of the mass of the droplet material $x(t)$ and the diameter of the deformed droplet $d(t)$ (see Fig. 1). In available experiments, the droplet "breakup" time has also been targeted, typically by Schlieren or shadowgraph imaging. Note that neither technique can unambiguously define the thermochemical state of the droplet at the "breakup" time. A coupled measurement for $x(t)$ and $d(t)$ yields the skin friction factor ϵ and the shape response factor ζ according to Eqs. 5 and 9, respectively, and in doing so, we determine the intrinsic vaporization time t_{v} in a more precise manner.

Skin friction correction describes the amplification of the flattened droplet diameter due to viscous drag around the periphery of the droplet. When momentum flux due to ballistic impact towards the droplet is small, peripheral viscous drag and hence, skin friction dominates. It follows that skin friction is important only in weak shocks. Therefore, we model ϵ as $\epsilon = \alpha/\mathrm{M}^{\beta}$, where M is the shock Mach number. The parameters α and β were fit to the experimental data from Ranger and Nicholls [1],

involving 2.7 mm water droplets and M = 1.5–3.5. The best fit yielded $\alpha = 1.01$ and $\beta = 1.94$. For simplicity, we model ϵ as $\epsilon = 1/\mathrm{M}^2$ henceforth. The fact that $\epsilon \sim 1/\mathrm{M}^2$ is not surprising, considering that the skin friction effect scales with the momentum flux of the post-shock flow. Comparisons of experimental displacement data for 2.7 mm water droplets against theoretical predictions, using Eq. 5 with $\epsilon = 1/\mathrm{M}^2$, are presented in Fig. 2(a) for several Mach numbers, including a sensitivity test for α at M = 2.1.

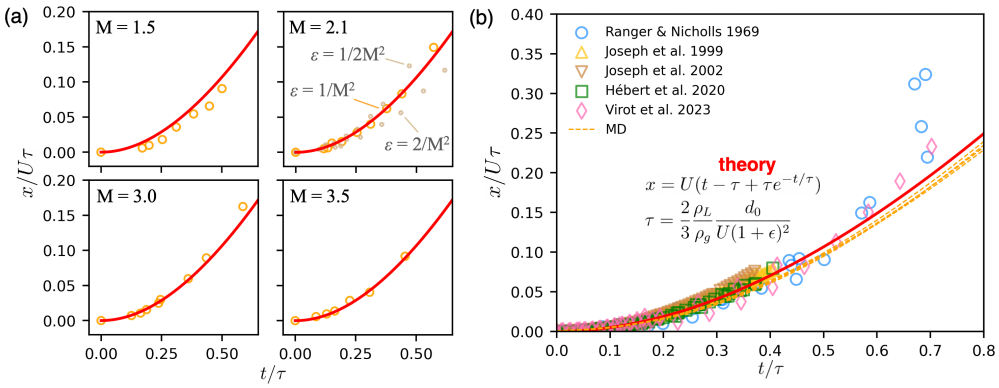

Figure 2: (a) Non-dimensional displacement against non-dimensional time for a 2.7 mm water droplet at several Mach numbers [1]. Theoretical predictions (Eq. 5 using $\epsilon = 1/\mathrm{M}^2$) are shown by the red lines. Sensitivity to ϵ is shown for M = 2.1. (b) Non-dimensionalized displacement measured experimentally (symbols, Ranger and Nicholls [1], Joseph et al. [6,7], Hébert et al. [2], and Virot et al. [3]); and from the MD data of Kateris et al. [5] (dashed lines with d_0 =10, 15, 20, and 25 nm), compared with prediction by Eq. 5 (red line).

Droplet displacements measured over ranges of droplet size, material, shock strength, and pre-shock conditions are expected to collapse into a single line when the absolute displacement and time upon shock passage are non-dimensionalized as given by Eq. 5 and shown in Fig. 2. Figure 2b collects all relevant data in a single chart. As it can be seen, the theory reproduces the data closely except for data of Ranger and Nicholls [1] at large t/τ values. The discrepancy is expected since the measurement relies on laser Schlieren which cannot identify the mass center, whereas the theory tracks the fuel center of mass. For the weak shocks used in those experiments, boundary layer stripping becomes relatively more important, causing the droplet centroid to be further downstream than the center of mass.

The shape response factor, ζ, may be obtained from Eq. 9. Figure 3 presents several sets of literature data ranging in droplet diameter d_0 from a few hundred μm to several mm, pre-shock pressure P_1 from 0.07 to 1 bar, shock strength from M = 1.5 to 10.7, and droplet materials from water to RP-2 (see Table 1 also). An inspection of Fig. 3 shows that for a given droplet material and pre-shock condition, the non-dimensionalization of time collapses the data into a single straight line, as expected. Values of the shape response factor ζ thus obtained across different experimental conditions are listed in Table 3. They exhibit sensitivity toward droplet material and pre-shock pressure.

A higher pre-shock pressure causes a higher post-shock pressure, and hence a greater amount of work is needed to flatten the droplet in the post-shock gas (thus smaller ζ). For instance, the 0.07 bar water data of [3] yielded a notably larger ζ value than that at 1 bar. Furthermore, the MD data [5] available at a pre-shock pressure of 7.1 bar yielded $\zeta = 0$, though the surface tension is also expected to play a role here: smaller droplets have greater surface energy and require a greater amount of work for flattening. Additional evidence for the role of surface tension comes from the RP-2 data of Schroeder et al. [4] at 0.14 bar; they yielded approximately the same value of ζ as the 0.07 bar water data of Virot et al. [3] Clearly, the low surface tension of RP-2 (*cf.*, 24.8 mN/m for n-dodecane vs. 71.7 mN/m for water at

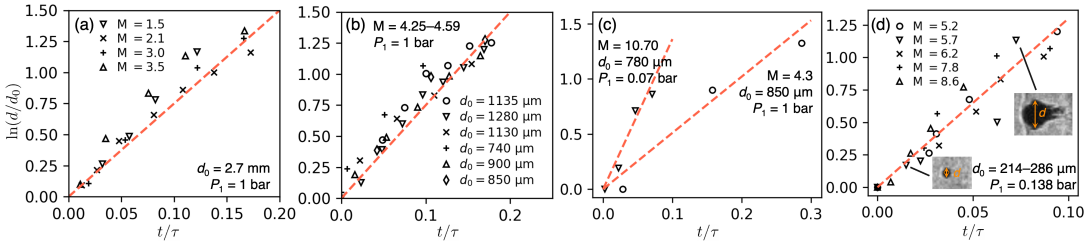

Figure 3: $\ln[d(t)/d_0)]_{t\to 0}$ as a function of non-dimensional time t/τ from experiments (symbols) by (a) Ranger and Nicholls [1] ($\zeta = 12$), (b) Hébert et al. [2] ($\zeta = 12$), (c) Virot et al. [3] (diamonds, $\zeta = 7.2$ and 24 for $P_1 = 1\,\mathrm{bar}$ and 70 mbar, respectively) and (d) Schroeder et al. [4] ($\zeta = 23$). A linear fit (dashed lines) of gradient $(\zeta + 3)/2$ between $\ln(d/d_0)$ and t/τ yields the shape response factor ζ.

300 K) allows an RP-2 droplet to flatten at the same rate as water at a lower pressure.

Table 1: Fuel, droplet size, shock strength, pre-shock pressure and resulting shape response factor values from experimental studies and from MD.

Case	fuel	d_0	M	P_1 (bar)	ζ
Ranger and Nicholls [1]	water	2.7 mm	1.5-3.5	1.0	12
Hébert et al. [2]	water	740–1550 µm	4.5	1.0	12
Virot et al. [3]	water	430–850 µm	4.5, 10.5	1.0, 0.07	7.2, 24
Schroeder et al. [4]	RP-2	214–286 µm	5.7-8.6	0.14	23
MD [5]	n-dodecane	10–25 nm	5.0	7.1	0

The ratio of the experimental breakup time $t_\mathrm{b}^\mathrm{obs}$ to the theoretical vaporization time t_v (Eq. 10) with ζ from Table 3 is compared with MD and experimental data in Fig. 4a over six orders of magnitude in droplet size, showing reasonably good agreement across different droplet materials, thermodynamic states and shock strengths. It should be noted that there was no deformation data available from [8] to extract ζ so a value of $\zeta = 2$ was assigned. Δh was calculated for each measurement. The agreement observed is expected, as both momentum and energy transfer mechanisms are the same across different length scales, liquid materials (water, n-dodecane, RP-2, JP-10), shock strengths (M = 1.5–11), and pre-shock thermodynamic conditions. The scatter in experimental data is expected, due to the lack of a rigorous definition for the "breakup" state, as discussed earlier. Figure 4b presents a band for theoretically predicted vaporization time (t_v) for typical liquid fuel (n-dodecane as the surrogate) at a pre-shock state of P_1 = 1 bar, T_1 = 300 K, impacted by a M = 5 shock. The edges of the band correspond to the extreme values of ζ for hydrocarbon fuels in Table 3. M = 5 MD data for n-dodecane, as well as M = 5 experimental data for RP-2 and JP-10 are included, with their measured vaporization time scaled by the ratio of experimental pressure to $P_1 = 1\,\mathrm{bar}$, thus accounting for the difference in ρ_g. The M = 5.7 RP-2 result from Schroeder et al. is also included, still showing reasonable agreement, despite the slight difference in shock Mach number.

Parameters ϵ and ζ are physics-based parameters that may be obtained from coupled experimental observations of time-dependent droplet displacement $x(t)$ and the flattened droplet diameter $d(t)$, as demonstrated above. The measurement of $d(t)$, in turn, yields the shape response factor ζ, which is required for making prediction for the intrinsic vaporization time t_v. The measurement of the "breakup" time can lead to large errors, since no existing technique can adequately measure the thermodynamic state of a liquid droplet in the post shock gas. Additional experiments are needed to determine the variation of the shape response factor as a function of droplet material, size, shock strength and pre-shock thermodynamic condition. Experimental difficulties remain in identifying the center mass of the droplet, which is probably better resolved through Raman spectroscopy than laser Schlieren or shadowgraph imaging.

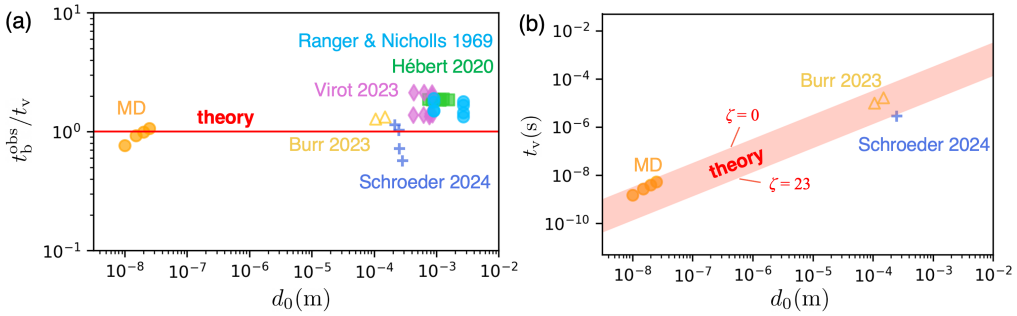

Figure 4: (a) The ratio of observed droplet breakup time to intrinsic vaporization time (Eq. 10) for the data of Ranger and Nicholls (circles) [1]; Hébert et al. (squares) [2]; Virot et al. (diamonds) [3]); Burr (triangles) [8]; Schroeder et al. (plus signs) [4]; and MD (orange circles) [5]. (b) Intrisic vaporization time for the range of ζ values observed across experiments and MD (Table 3) for n-dodecane at P_1 = 1 bar, T_1 = 300 K, M = 5. M = 5 MD and experimental data [5, 8] and M = 5.7 [4] included for comparison, after scaling ρ_g for P_1 = 1 bar.

4 Acknowledgment

The work was supported by the Office of Naval Research under Grant N00014-22-1-2606. ESG acknowledges support by the NSF Graduate Research Fellowship under Grant No. DGE-1656518.

References

[1] A. A. Ranger and J. A. Nicholls, "Aerodynamic shattering of liquid drops," *AIAA J.*, vol. 7, no. 2, pp. 285–290, 1969.

[2] D. Hébert, J. Rullier, J. Chevalier, I. Bertron, E. Lescoute, F. Virot, and H. El-Rabii, "Investigation of mechanisms leading to water drop breakup at mach 4.4 and Weber numbers above 10^5," *SN Appl. Sci.*, vol. 2, pp. 1–23, 2020.

[3] F. Virot, G. Tymen, D. Hébert, J. Rullier, and E. Lescoute, "Experimental investigation of the interaction between a water droplet and a shock wave above mach 4," *Shock Waves*, vol. 33, no. 5, pp. 369–383, 2023.

[4] S. Schroeder, S. Salauddin, A. Morales, M. Moran, R. Hytovick, E. Rigney, and K. Ahmed, "Deformation and aerobreakup of RP-2 droplets from hypersonic shock waves," *Proc. Combust. Inst.*, vol. 40, no. 1-4, p. 105338, 2024.

[5] N. Kateris, E. S. Genter, and H. Wang, "Shock-initiated fragmentation of n-dodecane nano-droplets: A molecular dynamics study," *29th ICDERS*, p. 268, 2023.

[6] D. D. Joseph, J. Belanger, and G. S. Beavers, "Breakup of a liquid drop suddenly exposed to a high-speed airstream," *Int. J. Multiph. Flow*, vol. 25, no. 6-7, pp. 1263–1303, 1999.

[7] D. D. Joseph, G. S. Beavers, and T. Funada, "Rayleigh–Taylor instability of viscoelastic drops at high Weber numbers," *J. Fluid Mech.*, vol. 453, pp. 109–132, 2002.

[8] J. R. Burr, "Detonation impacts on RP-2 droplets – experimental observations." MACCCR Annual Energy, Fuel and Combustion Research Review, 2023.